A molecular-dynamics study of the dynamic properties of liquid rubidium. II. Single-particle correlation functions

1994 J. Phys.: Condens. Matter 6 10923

(http://iopscience.iop.org/0953-8984/6/50/005)

J. Phys.: Condens. Matter 6 (1994) 10923–10937. Printed in the UK

A molecular-dynamics study of the dynamic properties of liquid rubidium: II. Single-particle correlation functions

G Kahl

Institut für Theoretische Physik, Technische Universität Wien, Wiedner Hauptstraße 8-10, A-1040 Wien, Austria

Received 18 February 1994, in final form 30 June 1994

Abstract. We present results for the dynamic single-particle correlation functions (i.e., the intermediate self-scattering function and the velocity autocorrelation function) of six liquid states of rubidium obtained in the same computer experiment as described in the preceding paper. Since the incoherent structure factor for Rb cannot be determined in a neutron-scattering experiment, our computer results could not be compared to experimental data. Temperature effects have been studied for both correlation functions: (i) an increasing temperature causes the single-particle correlations to decay much more rapidly than at low temperatures; (ii) the velocity autocorrelation function becomes a much more slowly decaying function in time. This reflects the cage (drift) effect encountered in dense (expanded) systems. An attempt to interpret the peak height and half-width of the self-dynamic structure factor in terms of mode-coupling theories has failed: either these subtle effects are encountered in a q-range inaccessible to computer experiment, or they require a more sophisticated analysis in terms of a *full* mode-coupling-theory approach. The diffusion constant extracted from the single-particle correlation functions shows good agreement with data obtained from the collective correlation functions, which marks a good internal consistency of the computer experiment.

1. Introduction

In the preceding paper [1] we discussed results for the dynamic *collective* correlation functions (CFs) of several states of liquid rubidium and a direct comparison between theoretical and experimental results; the present contribution is devoted to the dynamic *single-particle* CFs obtained in the same computer experiment. Due to the fact that the incoherent scattering length of Rb is smaller than the coherent scattering length by a factor of ten the determination of experimental data for the single-particle CFs of Rb is impossible: hence these dynamic CFs are available only in a computer experiment. However, we would like to mention that for several alkali metals the incoherent dynamic structure factor $S_s(q, \omega)$ can be measured (Na [2, 3, 4], Li [5, 6, 7]). The single-particle CFs considered here are the self-intermediate scattering function $F_s(q, t)$ (or its Fourier transform (FT) $S_s(q, \omega)$) and the velocity autocorrelation function (VACF) $\Psi(t)$.

On the theoretical side considerable effort has been made during the past years to construct models for the interpretation of single-particle CFs in terms of sophisticated theories. Besides the well known hydrodynamic (HF) and memory-function (MF) models [8, 9] (which turn out to describe the single-particle CFs far better than the collective CFs), several successful attempts have been made for first-principles models (e.g., [10, 11, 12, 13, 14, 15]). These theories start from the basic equations of statistical mechanics and finally arrive at expressions from which we learn that the MF of a dynamic CF is built up in a rather

0953-8984/94/5010923+15$19.50

complex way from all the other dynamic CFs, involving both single-particle and collective CFs (hence the name mode-coupling—MC—theories). Therefore, the determination of such an MF of a single-particle CF requires—e.g., in the formulation of Sjögren and Sjölander [11, 12]—the solution of a complex set of integral equations. In terms of these models it has become possible to explain several effects of single-particle CFs which were observed in particular in expanded systems: one example is the extremely slow decay of the VACF in time ($\Psi(t) \sim t^{-3/2}$) observed both for continuous [16] and hard-core potentials [17]. A closer analysis has revealed that this effect may be explained by the fact that a tagged particle builds up a vortex pattern of particles. A further example for an effect explained by MC theory is the deviation of the half-width of $S_s(q, \omega)$ from a purely diffusive behaviour for small q-values [10, 11, 12, 13, 14, 15]. Several of these effects have been assessed for neutron-scattering results [2, 18].

The aim of this paper is the presentation and discussion of results obtained in our computer experiment for the two single-particle CFs $F_s(q, t)$ and $\Psi(t)$. The study should primarily be considered as a completion to the preceding paper [1]. The data are interpreted in terms of HF and MF models. We do not interpret our data in terms of a *full* MC theory, as, e.g., by solving the complete set of MC equations as proposed by Sjögren [11, 12]; here we rather use results or predictions of MC theories to interpret our results, such as the behaviour of the half-width of $S_s(q, \omega)$ for small q-values or the long-time decay of the VACF in expanded systems. In particular, attention has been paid to temperature effects observed in the single-particle CFs caused by the variation of density and temperature along the coexistence curve of Rb. Using several models of the single-particle CFs we have extracted again the diffusion constant D and have compared it both to the experimental values [19] and to values obtained from the collective CFs in the preceding paper; this should also give us an idea of the internal consistency of the simulation.

Summarizing our results we have to admit that a simple analysis of our results in terms of expressions predicted by MC theory fails: neither the results predicted for the half-width and the ($\omega = 0$) value of the self-dynamic structure factor, nor the $t^{-3/2}$ decay of the VACF can be assessed with a sufficiently high reliability. Hence a more detailed analysis of the computer results in terms of a complete solution of the MC equations will be required. For the diffusion constant we obtained results of comparable accuracy as in the study on the collective properties, while the kinetic shear viscosity could not be extracted in a reliable way.

The paper is organized as follows: the following section contains only a few complementing remarks, in particular details of the single-particle CFs; characteristic parameters of the Rb states considered, of the simulation and of the pair interactions for this computer experiment have already been discussed in detail in section 2 of the preceding paper [1]. We present approximate cross-relations between the two single-particle CFs and several results predicted by MC theory which were used here for the interpretation of the computer data; we leave, however, a more complete presentation to the original papers. In the subsequent section we discuss our results for the single-particle CFs; one subsection therein is devoted to the diffusion constant and the kinetic shear viscosity. The paper is concluded with a summary.

2. The model, the simulation and the correlation functions

The single-particle CFs were obtained in the same molecular-dynamics (MD) computer experiment which we described in detail in the preceding paper [1]. Six Rb states (denoted

by I–VI) have been considered; the system parameters and a discussion of the interatomic forces may also be found in section 2 of [1]. The sets of q-vectors used in the study on the collective CFs have been extended by a further set of 16 q-vectors for each Rb state, all of them compatible with the periodic boundary conditions. These additional q-values were chosen to be rather in the small-q region: this choice should provide a better possibility of studying special effects predicted by MC theory in particular for the small-q range. The complete sets of q-vectors considered in this contribution are depicted for all Rb states in figure 1 of [1].

The single-particle CFs we have studied are the self-intermediate scattering function $F_s(q,t)$ and the normalized VACF $\Psi(t)$. The moments $\omega_s^n(q)$, ω_v^n and the Einstein frequency Ω_0^2 are defined in the usual way; the explicit expressions for these quantities in terms of the interatomic forces and static particle distribution functions up to fourth (ω_s^n) and second (ω_v^n) order are compiled in [20].

The time averaging has been performed in the same way as for the collective CFs by shifting origins (using the explicit expression of (7) of [20]): the CFs have been recorded every second time-step Δt over 2500 Δt-values (for Δt-values cf. table 1 in [1]). However, the difference in the time origins has now been chosen to be 2500 Δt, so that the events over which we average do not overlap. The resulting reduction in averaging events does not cause any loss in accuracy: an additional averaging over the number of particles compensates for it.

The dynamic single-particle CFs have again been studied in terms of HF and MF-n models (n representing the number of parameters involved); we use the same notation as in [20] and refer the reader for further details to this paper or standard text books [8, 9]. The only elastic property which may be extracted from the HF and MF models for the single-particle CFs is the diffusion constant D: it appears as a parameter in the HF model for $F_s(q,t)$ and may also be recovered from the long-wavelength limit of the relaxation time $\tau_s(q)$ of a second-order MF-1 *ansatz* for $F_s(q,t)$. From $\Psi(t)$, the diffusion constant may be obtained from the time integral of the VACF and finally the relaxation time τ_v of an MF model for $\Psi(t)$ is also related to D. In addition MC theory gives us in principle the possibility of determining the kinetic shear viscosity ν.

An *approximate* relation between the two single-particle CFs may be obtained as follows: we can write $F_s(q,t)$ in the so-called cumulant expansion

$$F_s(q,t) = \mathrm{e}^{-q^2\rho_1(t)+q^4\rho_2(t)-\ldots} \tag{1}$$

in terms of the functions $\rho_i(t)$, which may be related to the spatial moments [8]. Neglecting all terms beyond $\rho_1(t)$ (i.e., in the Gaussian approximation), one may derive the cross-relation

$$\Psi^G(t) = \frac{1}{v_0^2}\ddot{\rho}_1(t) \tag{2}$$

$v_0^2 = (\beta M)^{-1}$ being the thermal speed. For the half-width $\omega_s^{1/2}(q)$ and the ($\omega = 0$) value of the self-dynamic structure factor $S_s(q,\omega)$ the following behaviour has been predicted by MC theory for small q-values [21]:

$$S_s(q,0) = \frac{1}{\pi D q^2}[1 + a_1 q + a_2 q^2] \qquad \omega_s^{1/2}(q) = Dq^2[1 - b_1 q + b_2 q^2]. \tag{3}$$

The coefficients a_i and b_i are temperature dependent. For high temperatures we find a purely linear behaviour ('drift effect') for both quantities, as predicted in [13, 14, 15]: the

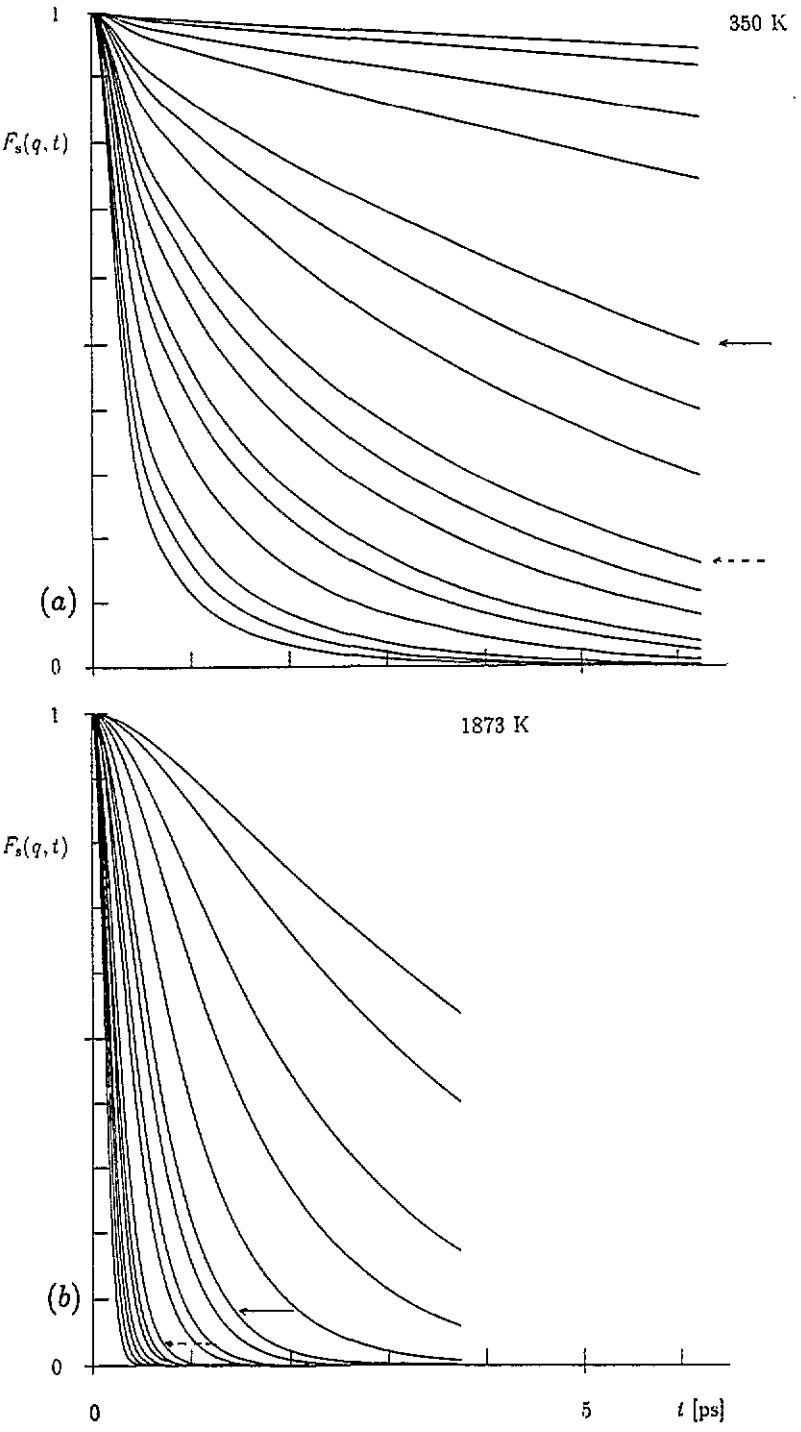

Figure 1. Self-intermediate scattering functions $F_s(q, t)$ as functions of q and t for the following Rb states: (a) I (350 K) and (b) VI (1873 K). The q-vectors are those (from top—smaller q-values to bottom—largest q-values) depicted in figure 1 of [1]. Curves for q-vectors near to 0.5 $Å^{-1}$ (1.0 $Å^{-1}$) are marked by a full (broken) arrow.

coefficients then contain D and ν as parameters. For low temperatures (where the 'cage effect' is predominant) a purely quadratic deviation from the linear behaviour is found by Wahnström and Sjögren [22]. For intermediate temperatures a crossover from a linear to a purely quadratic behaviour is predicted [21]. $\pi Dq^2 S_s(q,0)$ and $\omega_s^{1/2}(q)/Dq^2$ will be denoted by $[S_s(q,0)]_N$ and $[\omega_s^{1/2}(q)]_N$ respectively.

3. Results

3.1. The self-intermediate scattering function and the self-dynamic structure factor

Figure 1 shows the self-intermediate scattering function $F_s(q,t)$ for two selected temperatures (350 K and 1873 K). We observe that $F_s(q,t)$ decreases faster in time as we increase the temperature: e.g., for $q \sim 0.5$ Å^{-1} ($q \sim 1.0$ Å^{-1}) a factor of ~45 (~25) between 350 and 1873 K is observed.

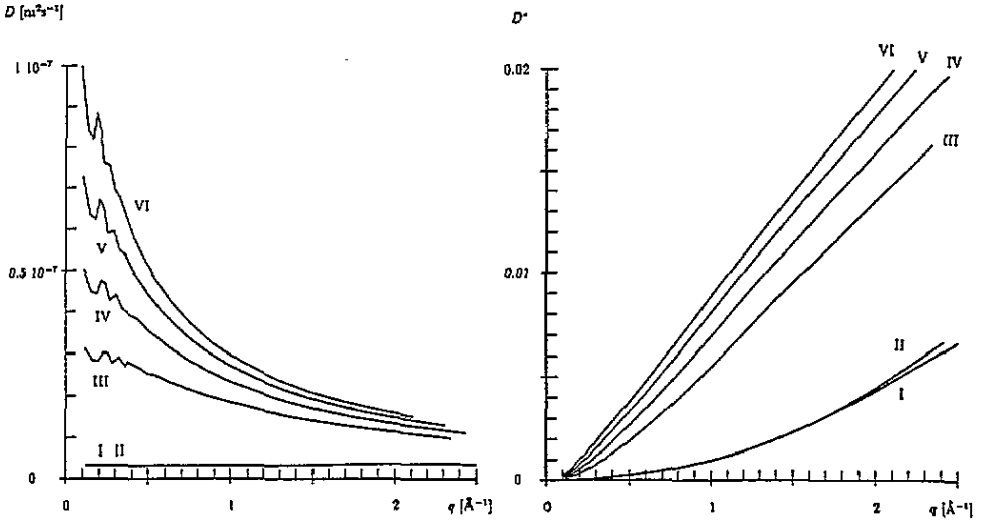

Figure 2. Generalized diffusion constant $D(q)$ and generalized dimensionless diffusion constant $D^*(q) = D(q)q^2\Delta t$ ($\Delta t = 3$ fs) as functions of q for Rb states I–VI obtained in an HF fit to $F_s(q,t)$.

The self-intermediate scattering functions have been fitted by means of an HF model (using a generalized diffusion constant $D(q)$ as a parameter) and an MF-1 model (parametrized by a relaxation time $\tau_s(q)$); for details cf. [20]. $D(q)$ is depicted as a function of q in figure 2. D may be recovered from $\tau_s(q)$ via $\lim_{q\to 0}\tau_s(q) = v_0^2/D\Omega_0^2$. Results for D obtained from the limits ($q \to 0$) of $\tau_s(q)$ and $D(q)$ are compiled in table 1. We obtain similar data for the diffusion constant as in the case of the preceding paper: up to state IV results are quite consistent (this also holds for the comparison with experiment [19]); for states V and VI larger differences are observed.

In contrast to the collective CFs, the half-width of the single-particle CF $F_s(q,t)$ shows no distinct structure near q_p: this is already clear from $D^*(q) = D(q)q^2$, which we obtained from the HF model for $F_s(q,t)$ and which is depicted in figure 2; in this model $\tau_s^{1/2}(q) = \ln 2/D^*(q)$ represents the half-width at half-maximum. $D^*(q)$ is monotonically

Table 1. Diffusion constant D in 10^{-8} m^2 s^{-1} as obtained via different methods from the computer experiment for Rb states I–VI: (a) HF fit to $F_s(q,t)$, (b) MF-1 fit to $F_s(q,t)$. The last column presents the values of the respective experimental values (p 845 in [19]; concerning their determination and their large error-bars cf. discussion in subsection 3.3 of the preceding paper [1]).

	D (m^2 s^{-1}) $\times$ 10^{-8}		
System	Theory (a)	Theory (b)	Experiment
I	0.325 ± 0.007	0.339 ± 0.007	0.352 ± 0.014
II	0.391 ± 0.003	0.406 ± 0.001	0.418 ± 0.020
III	3.320 ± 0.006	3.180 ± 0.006	3.661 ± 1.8
IV	5.540 ± 0.003	5.100 ± 0.003	6.047 ± 4.4
V	6.950 ± 0.004	7.560 ± 0.001	9.346 ± 8.4
VI	7.955 ± 0.005	10.80 ± 0.001	14.18 ± 14.7

increasing and does not show any particularities near q_p. This also holds (and the agreement is remarkably good) for the half-width of $F_s(q,t)$ obtained from the MF-1 model. We may conclude that the broadening of the collective CFs near q_p is an entirely collective effect.

We have compared the relaxation time $\tau_s(q)$ determined numerically in the MF-1 model with the prediction of the Lovesey model [23]

$$\tau_s^L(q) = \frac{1}{\gamma}(2\omega_0^2 + \Omega_0^2)^{-1/2}. \tag{4}$$

The coefficient γ is obtained in the low-q limit and is given by $\Omega_0 D/v_0^2$. We know by now that the determination of D is a rather delicate task and hence small deviations in this quantity might influence the value of γ, and consequently $\tau_s^L(q)$. In order to guarantee a proper comparison between $\tau_s(q)$ and $\tau_s^L(q)$ we proceeded as follows: γ in (4) has been adjusted to obtain agreement between $\tau_s^L(q)$ and $\tau_s(q)$ for the smallest q-vector. In fact the resulting D-values ($D = v_0^2\gamma/\Omega_0$) do not differ too much from those reported in [1]: they agree very well with the results of an HF fit to $F(q,t)$ (cf. table 5 of [1]). Our γ-values range from 0.57 (state I) to 1.992 (state VI) and differ quite strongly from the ideal-gas limit (i.e., $\gamma \sim 2/\sqrt{\pi} \sim 1.13$). The results for $\tau_s(q)$ and $\tau_s^L(q)$ are depicted in figure 3: we see immediately that for the single-particle CFs not only quantitative but also substantial qualitative differences are observed; we remind the reader that in the case of the collective CFs a nice agreement was found. Again, the results for the relaxation times for states I and II are clearly separated, while the curves for states III–VI are rather close, despite the large temperature range they cover.

Turning towards the self-structure factor $S_s(q,\omega)$ we have depicted in figures 4 and 5 the normalized ($\omega = 0$) value of $S_s(q,\omega)$ and the normalized half-width $\omega_s^{1/2}(q)$ as functions of q. These data have been calculated from our MF-1 and HF fit parameters. The D-value required in the normalization procedure as defined above is the average over the extrapolations of $\omega_s^{1/2}(q)$ and $S_s(q,0)$ towards zero. In this way we obtain two different results for D, one from the HF, the other from the MF-1 route. These D-values are compiled in table 2. It is worthwhile to mention that the error-bars are rather small, which indicates a good internal consistency of the different results obtained via the $S_s(q,\omega)$ and the $\omega_s^{1/2}(q)$ routes. On the other hand data calculated from the HF and the MF-1 model show discrepancies up to 1673 K, which can be considered as acceptable, while data differ substantially for 1873 K. We have then fitted the results for $S_s(q,0)$ and $\omega_s^{1/2}(q)$ to the

Table 2. Diffusion constant D in 10^{-8} m^2 s^{-1} as obtained from an expression predicted by MC theory for $S_s(q,\omega)$ and $\omega_s^{1/2}(q)$ (cf. text and equation (3)); the represented values are obtained from (a) HF and (b) MF-1 parametrization of $F_s(q,t)$. Every value represents an average over the data obtained via equation (3).

	D (m^2 s^{-1}) × 10^{-8}	
System	(a) HF	(b) MF-1
I	0.327 ± 0.000 02	0.319 ± 0.0003
II	0.404 ± 0.000 02	0.397 ± 0.0003
III	3 346 ± 0.0024	3.485 ± 0.024
IV	5.715 ± 0.029	5.992 ± 0.11
V	8.698 ± 0.20	8.243 ± 0.14
VI	12.662 ± 0.74	9.308 ± 0.10

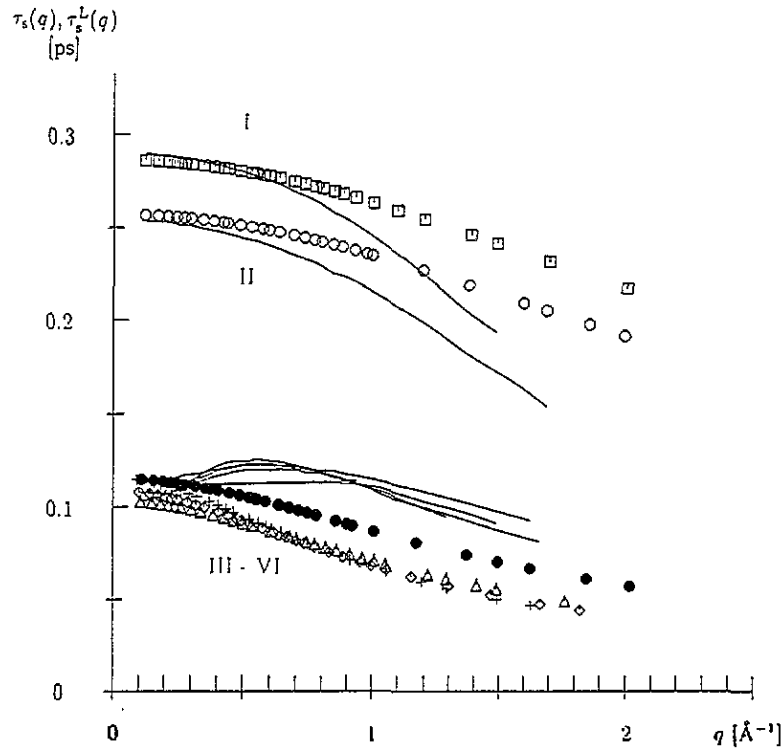

Figure 3. Relaxation time $\tau_s(q)$ of an MF-1 parametrization of the self-intermediate scattering function $F_s(q,t)$ and the corresponding Lovesey value $\tau_s^L(q)$ [23] as functions of q for Rb states I–VI. Symbols are as in figure 8(b) of [1].

general quadratic expressions (3); the normalized data $[S_s(q,0)]_N$ and $[\omega_s^{1/2}(q)]_N$ (D in the normalizing factor see above) are displayed in figures 4 and 5 as symbols, while the analytic expressions are shown as full and broken lines. Up to ~1 Å^{-1} the results for the HF and the MF-1 branches are within good numerical agreement (note the different vertical scale for states I, II and III to VI). Discrepancies for larger q-values mark the limit of validity of the hydrodynamic model. Since we observe for the absolute values a very good agreement, the *quantitative* differences for the $[S_s(q,0)]_N$-curves for states V and VI may

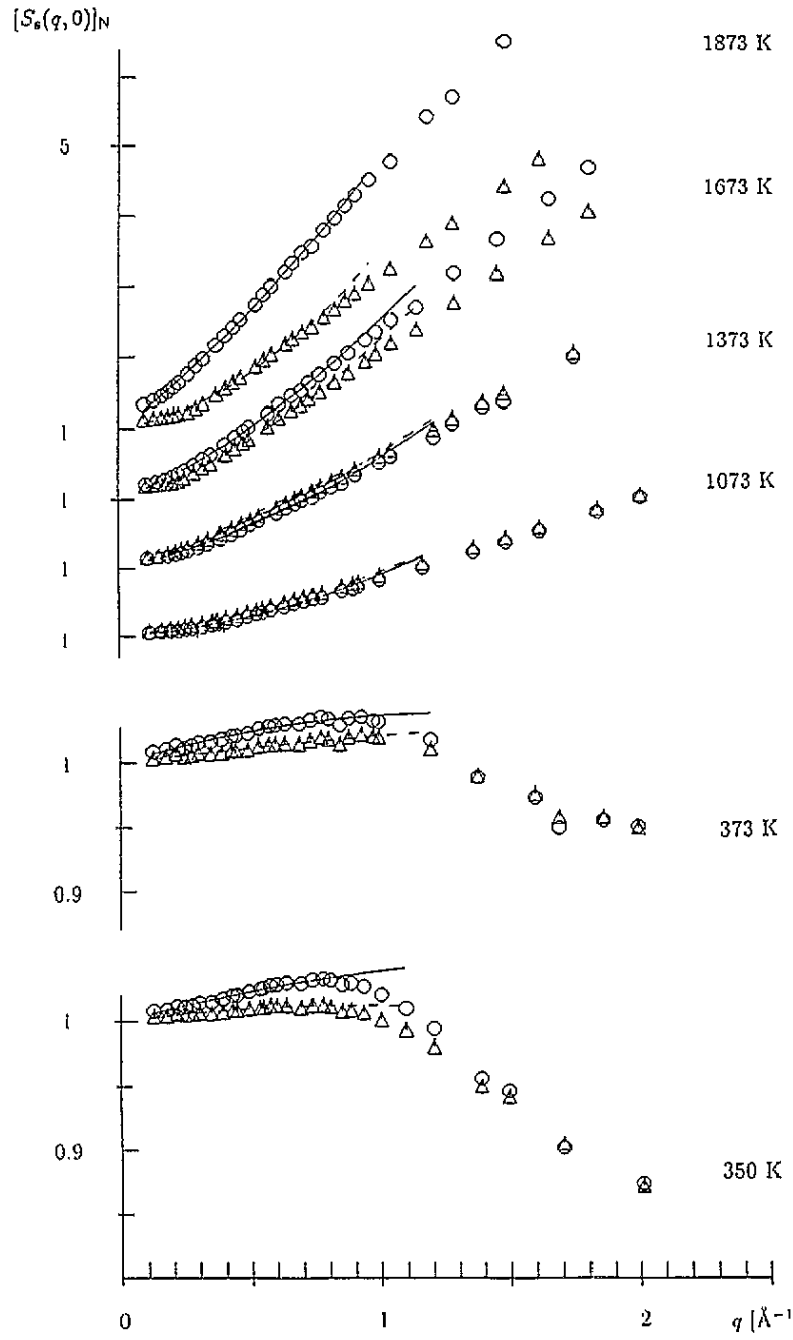

Figure 4. Normalized ($\omega = 0$) value $[S_s(q,\omega)]_N$ of the self-dynamic structure factor $S_s(q,\omega)$ (cf. text) as a function of q for Rb states I–VI as obtained from an HF (○) and an MF-1 (△) fit to $F_s(q,t)$. The curves indicate quadratic functions obtained in a least-squares fit to the data (full line: HF, broken line: MF-1 model).

be explained by different D-values in the above normalization prescription (cf. table 2).

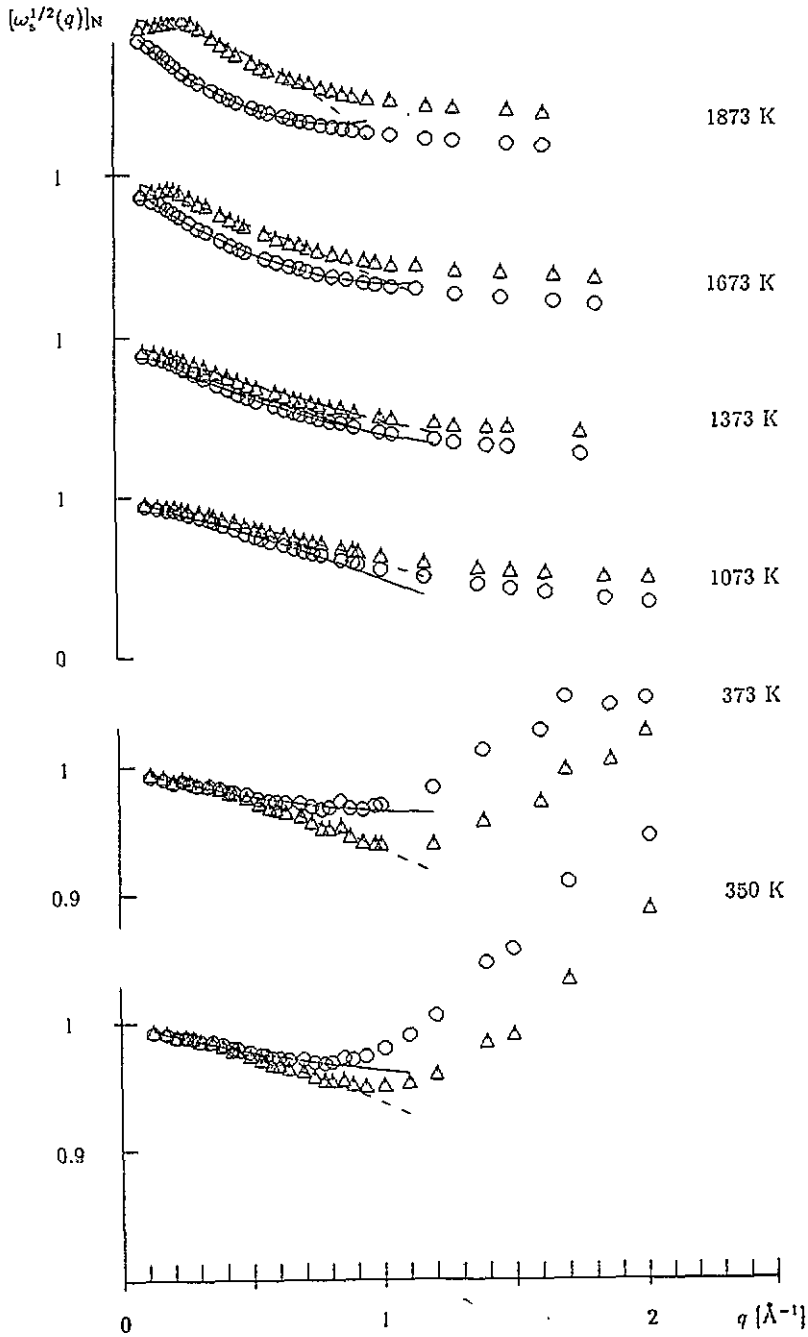

Figure 5. Normalized half-width $[\omega_s^{1/2}(q)]_N$ of the self-dynamic structure factor $S_s(q,\omega)$ (cf. text) as a function of q for Rb states I–VI as obtained from an HF (○) and an MF-1 (△) fit to $F_s(q,t)$. The curves indicate quadratic functions obtained in a least-squares fit to the data (full line: HF, broken line: MF-1 model).

Data for $[\omega_s^{1/2}(q)]_N$ show *qualitative* differences for the higher temperatures, a consequence

of an internal inconsistency.

The simulation data have been adjusted to the general full quadratic expressions (3) with q-values ranging up to ~ 1 Å^{-1}. Using the parameters a_i and b_i obtained in this fit we have then tried to interpret our data in terms of models proposed by MC theory. We have to admit that the accuracy of our data analysis is obviously not sufficiently high to allow the verification of the predicted behaviour: no clear temperature trends of the coefficients a_i and b_i, $i = 1, 2$ could be observed; their values depend furthermore in a sensitive way on the number of q-values included in the fit. One possible explanation for these problems might also be that these effects are only encountered in a q-range which is not accessible for a computer experiment of that sample size. It is, however, more probable that such a simple interpretation of the data is not sufficient: only a detailed analysis in terms of a *complete* MC approach (where these coefficients are expressed in terms of special functions introduced in the different MC formalisms [11, 12, 13, 14, 15, 21]) can give a final and more conclusive decision if computer experiments are in fact accurate enough to describe these subtle effects predicted by MC theory. As a consequence we cannot consider results for the kinetic shear viscosity obtained in the high-temperature range as reliable and therefor we will not present them here.

3.2. The velocity autocorrelation function

Figure 6 shows the VACF $\Psi(t)$ for Rb states I–VI investigated in this study. For low temperatures we observe a behaviour which may be understood very well in terms of the so-called 'cage effect', i.e., a tagged particle is enclosed—due to the high density—in a cage formed by the other particles. Within this cage it can propagate only over short distances, it will be reflected (expressed by negative values of $\Psi(t)$) and finally will quickly lose the memory of its initial velocity (i.e., the VACF will decay quickly in time). As we increase the temperature, the cages will become larger and finally will disappear and the particles can propagate over larger distances without any collisions, which is expressed in a slower decay of the VACF in time: indeed we find an extremely slow decay for 1873 K. This behaviour has been investigated more closely for two model systems, i.e., for hard spheres [17] and for repulsive Lennard-Jones systems [16] where it was found that in fact $\Psi(t)$ decays as $t^{-3/2}$ for large t. The picture behind these results was revealed by Alder and Wainwright [17] by studying the velocity field around a tagged particle: the authors found that particles in front of and behind this particle tend to acquire velocities in the same direction as the tagged particle, so that particles in front are pushed and those behind are drawn. The result is a vortex pattern around the tagged particle and the velocities decay solely due to the influence of the shear viscosity. These findings were substantiated by hydrodynamic [24, 25] and MC-theory [15, 26] models.

In order to visualize these predictions one has to plot $[\log \Psi(t)]$ against $[\log t]$ and should then obtain in particular for intermediate and higher temperatures a straight line with a slope of $-\frac{3}{2}$. We present these results in figure 7: only for the intermediate temperatures (states III and IV) can we claim that there is some similarity with such a straight line while for the highest temperatures a clear curvature is observed, which indicates that the VACF decays even more slowly than predicted. Looking for possible reasons we have compared LJ and liquid-metal potentials: Rb potentials are explicitly state dependent and they are in reduced units—in contrast to LJ systems—still of about the same depth as near the melting point. We have therefore performed additional simulations for states V and VI, where we have used instead of the full interaction only the repulsive part (those states are denoted by V′ and VI′): we used a potential which has been truncated at the position of the first minimum (in the sense of Weeks, Chandler and Andersen [27]) and shifted so that the new

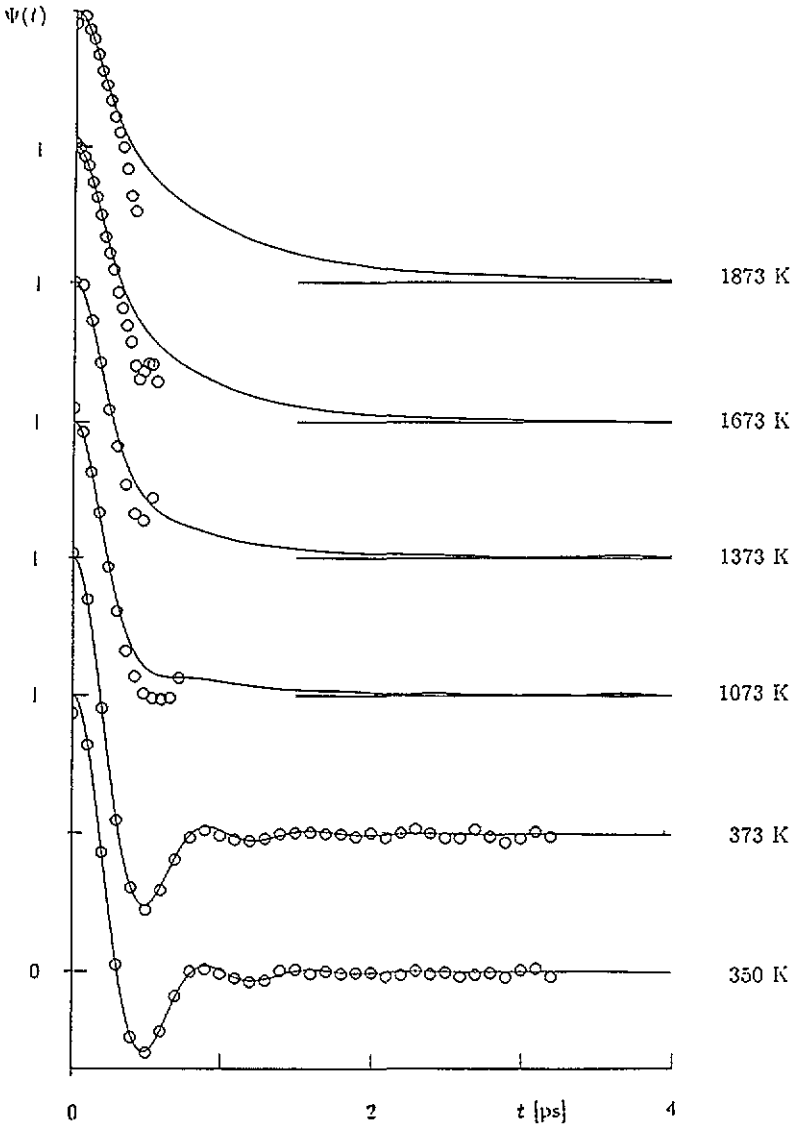

Figure 6. Normalized VACF $\Psi(t)$ (full lines) and $\Psi^{G}(t)$ (obtained from the Gaussian approximation to $F_s(q,t)$; symbols) as functions of t for Rb states I–VI.

potential merges smoothly into the abscissa. Results are also presented in figure 7 by the broken line: although for these systems the curvature of $\Psi(t)$ is less pronounced than for the full potential we still observe a similar behaviour which excludes the strong attractive potential as the only possible explanation. Other possible reasons for the deviation from the predicted behaviour might be (i) the rather *low* density (while the results for the repulsive LJ system were obtained at *intermediate* densities); (ii) the softer repulsion of liquid-metal potentials compared to LJ interactions. To settle this question unambiguously would require more complete calculations or—still better—an interpretation of our computer simulation data in terms of a complete MC-theory approach. We hope to answer this question in the near future.

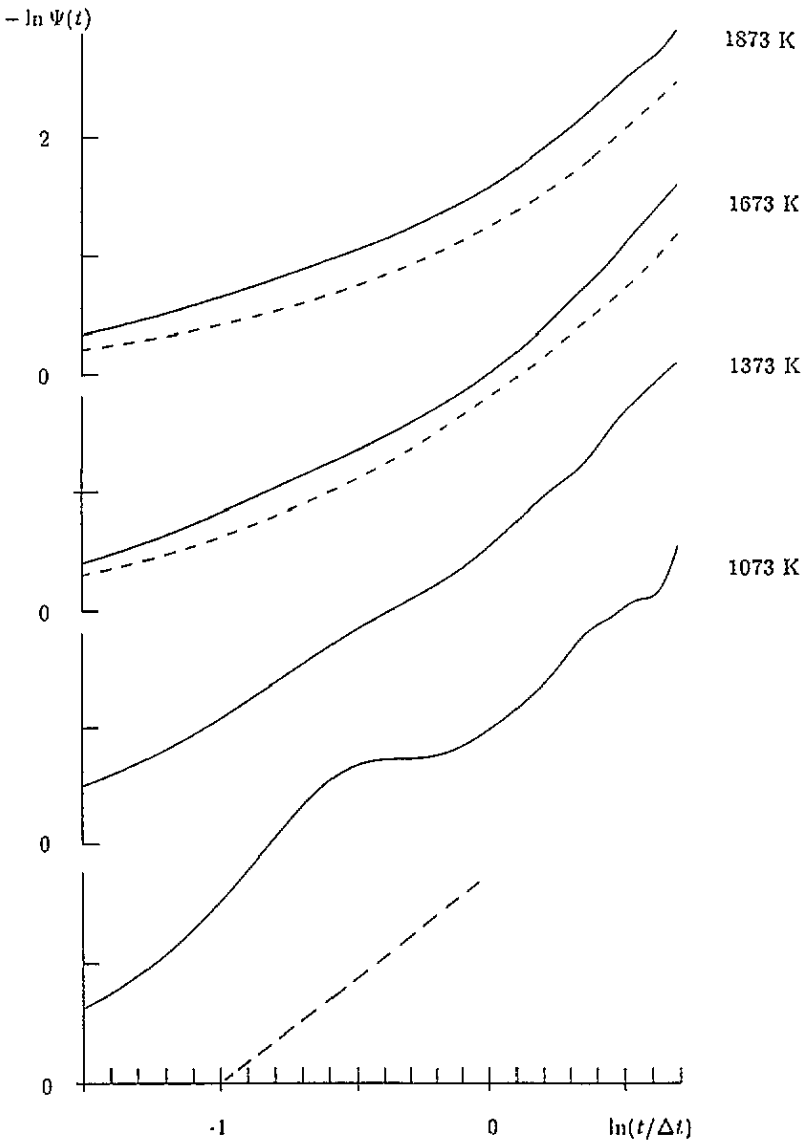

Figure 7. Log–log plot of the VACF (i.e., $\log[\Psi(t)]$ against $\log[t]$; $\Delta t = 1$ ps): full line, Rb states III–VI; broken line, the repulsive systems V′ and VI′ (as defined in the text). The broken straight line indicates the results predicted by MC theory [15, 26], i.e., $\log[\Psi(t)] \sim t^{-3/2}$.

Finally we have analysed our data in terms of the Gaussian approximation. In figure 6 we show the VACF $\Psi(t)$ calculated in the computer experiment along with $\Psi^{G}(t)$ as obtained from our results of $F_s(q, t)$ via (2). While agreement between the approximate and exact function is convincing for the lowest temperatures (as it was also for Cs [20, 28]), we find increasing discrepancies even for intermediate temperatures. This reveals that the contribution of the higher-order spatial moments in the cumulant expansion (2) become increasingly important as we expand the system.

3.3. Thermodynamic and elastic properties

Using the HF and the MF-1 models for the single-particle CFs we can only extract—as outlined in section 2—the diffusion constant D. Results for this quantity obtained in different ways are compiled in tables 1–3, along with the experimental values [19]. Concerning the determination of these experimental data and the comparatively large error-bars for higher temperatures we refer the reader to a discussion in the preceding paper [1].

(i) Results obtained from both models for $F_s(q, t)$ are up to intermediate temperatures in good agreement with D-data calculated from the mean square displacement (table 5 of [1]). For states V and VI rather substantial differences are observed.

(ii) The same holds for the D-data obtained from the extrapolation towards zero of the half-width $\omega_s^{1/2}(q)$ and $S_s(q, 0)$: in addition, for states V and VI the internal consistency breaks down, i.e., results obtained from the two routes differ substantially (~25 %).

(iii) Finally, D as determined from the time integral of the VACF and an MF fit to $\Psi(t)$ yields a good internal consistency and good agreement with the data from the mean square displacement. In particular good agreement of the MF value is the more astonishing, since it is well known that the MF model is not able to describe the VACF accurately [20].

As a consequence of our problems with the MC approach described above we do not present results for the kinetic shear viscosity ν here.

Table 3. Diffusion constant D in 10^{-8} m^2 s^{-1} as obtained via different methods from the computer experiment for Rb states I–VI: (a) time integral of the VACF (cf. (26) of [20]) and (b) MF-1 fit to $\Psi(t)$. The last column presents the respective experimental values (p 845 in [19]; concerning their determination and the large error-bars cf. discussion in subsection 3.3 of the preceding paper [1]).

	D (m^2 s^{-1}) × 10^{-8}		
System	Theory (a)	Theory (b)	Experiment
I	0.298	0.425	0.352 ± 0.014
II	0.454	0.526	0.418 ± 0.020
III	3.429	3.014	3.661 ± 1.8
IV	5.675	5.048	6.047 ± 4.4
V	8.483	7.994	9.346 ± 8.4
VI	12.303	11.515	14.18 ± 14.7

4. Conclusion

We have reported on results of the single-particle CFs of liquid Rb; the temperature ranges from near the melting point up into the critical region. Due to the fact that the incoherent structure factor cannot be measured for Rb direct comparison with experiment was not possible. For these CFs several interesting effects have been predicted by MC theory. From the present results we can learn that only some of these predictions can be verified from an interpretation of data from a computer experiment at a level as we have used it with a sufficiently high accuracy and reliability. Both the 'cage effect' (dominant at low temperatures) and the 'drift effect' (dominant at high temperatures) could be reproduced nicely in a qualitative way; however, the predicted $t^{-3/2}$ decay of the velocity autocorrelation

function for high temperatures could not be verified. In our experiment this function decays even more slowly in time. In a similar way the predicted q-dependence of the half-width and the $(\omega = 0)$ value of the self-dynamic structure factor $S_s(q, \omega)$ could not be verified from our data with a sufficiently high accuracy; several reasons for this failure have been considered: this might be due to the fact either that the accuracy of the computer experiment is simply not high enough or that these effects are only encountered for very small q-values which are inaccessible to our experiment. In any case an analysis of the data in terms of a full MC approach has become absolutely necessary to settle these questions unambiguously: then the quantities which appear as parameters in these expressions can be written in terms of special functions of the MC formalism and should give numerically more reliable results. The diffusion constant, extracted via several routes from the models fitted to the computer data shows an agreement of about the same degree as encountered in the case of the collective correlation functions. Again the internal consistency is—except for the highest temperatures—quite satisfactory. Due to the problems mentioned above the results for the kinetic shear viscosity are unreliable.

Acknowledgments

The author would like to thank Professor J Hafner (Wien) for many interesting and stimulating discussions and useful hints. This work was supported by the Österreichische Forschungsfonds under project No P8912-PHY and the Oesterreichische Nationalbank under project No 4649. Computational aid by Drs S Kambayashi and G Nowotny is gratefully acknowledged. The author would like to thank Dr C Morkel (Garching) and Dr L Sjögren (Göteborg) for useful discussions; he is in particular indebted to Dr Sjögren for communicating unpublished results [21].

References

[1] Kahl G and Kambayashi S 1994 *J. Phys.: Condens. Matter* **6** 10 897
[2] Montfroy W, de Schepper I M, Bosse J, Gläser W and Morkel C 1986 *Phys. Rev.* A **33** 1405
[3] Morkel C and Gläser W 1986 *Phys. Rev.* A **33** 3383
[4] Morkel C, Gronemeyer C, Gläser W and Bosse J 1987 *Phys. Rev. Lett.* **58** 1873
[5] de Jong P H K, Verkerk P, Ahda S and de Graaf L A 1992 *Recent Development in the Physics of Fluids* ed W S Howells and A K Soper (Bristol: Hilger) p F233
[6] de Jong P H K, Verkerk P and de Graaf L A 1993 *J. Non-Cryst. Solids* **156–158** 48
[7] de Jong P H K 1993 *PhD Thesis* Delft
[8] Boon J-P and Yip S 1980 *Molecular Hydrodynamics* (New York: McGraw-Hill); 1991 *Molecular Hydrodynamics* (New York: Dover)
[9] Hansen J-P and McDonald I R 1986 *Theory of Simple Liquids* 2nd edn (London: Academic)
[10] Götze W and Zippelius A 1976 *Phys. Rev.* A **14** 1842
[11] Sjögren L and Sjölander A 1979 *J. Phys. C: Solid State Phys.* **12** 4369
[12] Sjögren L 1980 *J. Phys. C: Solid State Phys.* **13** 705
[13] Bedeaux D and Mazur P 1974 *Physica* **73** 431
[14] de Schepper I M, van Beyren H and Ernst M H 1974 *Physica* **75** 1
[15] de Schepper I M and Ernst M H 1979 *Physica* A **98** 189
[16] Levesque D and Ashurst W T 1974 *Phys. Rev. Lett.* **33** 977
[17] Alder B J and Wainwright T E 1970 *Phys. Rev.* A **1** 18
[18] Verkerk P, Builtjes J H and de Schepper I M 1985 *Phys Rev.* A **31** 1731
[19] Ohse R 1985 (ed) *Handbook of Thermodynamic and Transport Properties of Alkali Metals* (Oxford: Blackwell)
[20] Kambayashi S and Kahl G 1992 *Phys. Rev.* A **46** 3255

[21] Sjögren L 1993 Private communication
[22] Wahnström G and Sjögren L 1982 *J Phys. C: Solid State Phys.* **15** 401
[23] Copley J R D and Lovesey S W 1975 *Rep. Prog Phys.* **38** 461
[24] Ernst M H, Hauge E H and van Leeuwen J M J 1970 *Phys. Rev. Lett.* **25** 1254
[25] Ernst M H, Hauge E H and van Leeuwen J M J 1971 *Phys. Rev.* A **4** 2055
[26] Dorfman J R and Cohen E G D 1972 *Phys. Rev.* A **6** 776
[27] Weeks J D, Chandler D and Andersen H C 1971 *J. Chem. Phys.* **54** 5237
[28] Kahl G, Kambayashi S and Nowotny G 1993 *J. Non-Cryst. Solids* **156–158** 15